Baryon magnetic moments in a QCD-based quark model with loop corrections

Phuoc Ha* and Loyal Durand†
Physics Department, University of Wisconsin-Madison, Madison, Wisconsin 53706
(Received 24 April 1998; published 25 September 1998)

We study meson loop corrections to the baryon magnetic moments starting from a QCD-based quark model derived earlier in a quenched approximation to QCD. The model reproduces the standard quark model with extra corrections for the binding of the quarks. The loop corrections are necessary to remove the quenching. Our calculations use heavy baryon perturbation theory with chiral baryon-meson couplings, the quark model moment couplings, and a form factor characterizing the structure of baryons as composite particles. The form factor reflects soft wave function effects with characteristic momenta ≈ 400 MeV, well below the usual chiral cutoff of ≈ 1 GeV. The resulting model involves only three parameters, the quark moments μ_u and μ_s, and a parameter λ that sets the momentum scale in the wave functions. We find that this approach substantially improves the agreement between the theoretical and experimental values of the octet baryon magnetic moments, with an average difference between the theoretical and experimental moments of $0.05\mu_N$. An extension to the decuplet states using the same input predicts a moment of $1.97\ \mu_N$ for the Ω^- hyperon, in excellent agreement with the measured moment of $2.02 \pm 0.05\ \mu_N$. [S0556-2821(98)06521-7]

PACS number(s): 13.40.Em, 11.30.Rd

I. INTRODUCTION

The simple, nonrelativistic quark model (QM) gives a qualitatively good description of the baryon moments. Under the assumption that each baryon is composed of three valence or constituent quarks in a state with all internal orbital angular momenta equal to zero, the moments are given by expectation values of the spin moment operators

$$\boldsymbol{\mu}^{QM} = \sum_{\mathrm{q}} \mu_{\mathrm{q}} \boldsymbol{\sigma}_{\mathrm{q}}, \tag{1.1}$$

leading to the standard expressions

$$\mu_p^{QM} = \frac{1}{3}(4\mu_u - \mu_d), \ldots, \quad \mu_q = \frac{e_q}{2m_q}, \tag{1.2}$$

where the effective quark moments $\mu_u = -2\mu_d$ and μ_s can be treated as free parameters in attempting to fit the data. The predicted pattern of the signs for the moments agrees with observation. A least-squares fit to seven measured octet moments (the transition moment $\mu_{\Sigma^0\Lambda}$ is left to be predicted) gives a root-mean-square deviation of theory from experiment of $0.12\ \mu_N$, about 11% of the average magnitudes of the moments. Agreement at this level can be regarded as an outstanding success of the quark model, but the deviations also give a very sensitive test of baryon structure. There is presently no completely successful first-principles theory of the moments.

In this paper, we approach the moment problem dynamically using a QCD-based quark model [1] with meson loop corrections. The model has only three parameters, namely the quark moments $\mu_u = -2\mu_d$ and μ_s, and a parameter λ that characterizes the momentum scale of meson-baryon interactions, with the particles regarded as composite. We find that this approach reduces the average deviation of the calculated moments from experiment to $0.05\mu_N$, a substantial improvement, and that the loop corrections are small compared to the leading QM terms, suggesting reasonable convergence for the loop expansion.

A different approach to the moment problem using chiral perturbation theory (ChPT) with loop corrections has been studied recently by a number of authors. Excellent fits to the data can be obtained for either conventional [2–5] or a modified [6] chiral counting. However, as pointed out elsewhere [7], the general fits are essentially independent of the dynamical input, and are best thought of as giving parametrizations of the data. In particular, the introduction of the counterterms needed to eliminate divergences in the loop integrals results in the appearance of five new chiral couplings [2,5,6] at the one-loop level in addition to the two tree-level [8] couplings. The seven well-measured octet moments can be fitted exactly using these seven parameters, whether or not the calculated loop corrections are included [7]. The theory is only weakly predictive with respect to the remaining quantity, the $\Sigma^0\Lambda$ transition moment, which is not known precisely. Furthermore, the loop corrections in ChPT are nearly as large as the tree-level terms, and convergence of the expansion is at best slow, when the divergences are regularized using dimensional regularization. This problem is not unexpected, since chiral symmetry is known to be badly broken for the baryons. The remaining predictions [2–4] are sum rules that can be motivated by large N_c expansions or expansions in the symmetry breaking mass parameter m_s in ChPT, but do not depend explicitly on the dynamics.

Our intent here is to present a dynamical approach to the baryon moments in which we emphasize the composite nature of the baryons and use a description based on the QM rather than the chiral picture. We begin in Sec. II by reviewing briefly the derivation of the QM, with corrections, from QCD using a Wilson-loop approach [1]. The derivation involves the suppression of internal quark loops (''quenching''), an approximation that is likely to account for the de-

*Electronic address: phuoc@theory1.physics.wisc.edu
†Electronic address: ldurand@theory2.physics.wisc.edu

ficiencies of the resulting model. The addition of quark loops necessary to remove the quenching introduces meson loops when the theory is viewed at the hadron level [1], and the effect of these loops on the baryon moments must be considered. We develop our approach to loop effects in Sec. III, where we define the couplings we will use for low momentum meson-baryon and electromagnetic interactions in a calculation based on heavy-baryon perturbation theory [9,10]. We also introduce the form factor needed to account for the extended structure of the baryons and mesons viewed as composite particles. We present our final expression for the octet moments, the results of our numerical analysis, and our conclusions in Sec. IV. Finally, we give the detailed results needed to evaluate the formal expressions for the moments in two appendices.

II. BARYON MOMENTS IN A QCD-BASED QUARK MODEL

A. Background

In previous work [1], we analyzed the QM for the baryon moments in the context of QCD. Our approach was based on the work of Brambilla *et al.* [11], who derived the interaction potential and wave equation for the valence quarks in a baryon from QCD using a Wilson-line construction. Their basic idea was to construct a Green's function for the propagation of a gauge-invariant combination of quarks joined by path ordered Wilson-line factors

$$U = P \exp ig \int A_g \cdot dx, \tag{2.1}$$

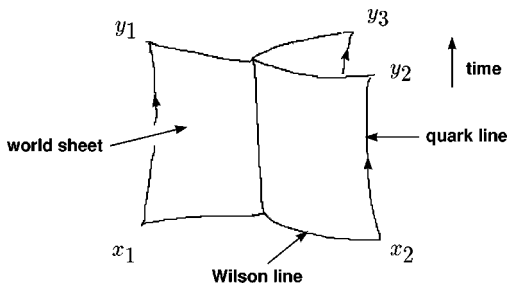

FIG. 1. World sheet picture for the structure of a baryon in the Wilson-loop approach.

where A_g is the color gauge field. The Wilson lines sweep out a three-sheeted world sheet of the form shown in Fig. 1 as the quarks move from their initial to their final configurations.

By making an expansion in powers of $1/m_q$ using the Foldy-Wouthuysen approximation, and considering only forward propagation of the quarks in time, Brambilla *et al.* were able to derive a Hamiltonian and Schrödinger equation for the quarks, with an interaction which involves an average over the gauge field. That average was performed using the minimal surface approximation in which fluctuations in the world sheet are ignored, and the geometry is chosen to minimize the total area of the world sheet subject to the motion of the quarks. The short-distance QCD interactions were taken into account explicitly. Finally, the kinetic terms could be resummed. The result of this construction is an effective Hamiltonian [11] to be used in a semirelativistic Schrödinger equation $H\Psi = E\Psi$:

$$H = \sum_i \sqrt{p_i^2 + m_i^2} + \sigma(r_1 + r_2 + r_3) - \sum_{i<j} \frac{2}{3}\frac{\alpha_s}{r_{ij}} - \frac{1}{2m_1^2}\frac{\sigma}{r_1}\mathbf{s}_1 \cdot (\mathbf{r}_1 \times \mathbf{p}_1) + \frac{1}{3m_1^2}\mathbf{s}_1 \cdot \left((\mathbf{r}_{12} \times \mathbf{p}_1)\frac{\alpha_s}{r_{12}^3} + (\mathbf{r}_{13} \times \mathbf{p}_1)\frac{\alpha_s}{r_{13}^3} \right)$$

$$- \frac{2}{3}\frac{1}{m_1 m_2}\frac{\alpha_s}{r_{12}^3}\mathbf{s}_1 \cdot \mathbf{r_{12}} \times \mathbf{p}_2 - \frac{2}{3}\frac{1}{m_1 m_3}\frac{\alpha_s}{r_{13}^3}\mathbf{s}_1 \cdot \mathbf{r_{13}} \times \mathbf{p}_3 + \cdots . \tag{2.2}$$

Here $\mathbf{r}_{ij} = \mathbf{x}_i - \mathbf{x}_j$ is the separation of quarks i and j, r_i is the distance of quark i from point at which the sum $r_1 + r_2 + r_3$ is minimized, and $\mathbf{p}_i$ and $\mathbf{s}_i$ are the momentum and spin operators for quark i. The parameter σ is a ''string tension'' which specifies the strength of the long range confining interaction, and α_s is the strong coupling. The terms hidden in the ellipsis include tensor and spin-spin interactions which will not play a role in the analysis of corrections to the moment operator, and the terms that result from permutations of the particle labels. The full Hamiltonian is given in [11]. This Hamiltonian, including the terms omitted here, gives a good description of the baryon spectrum as shown by Carlson, Kogut, and Pandharipande [12] and by Capstick and Isgur [13], who proposed it on the basis of reasonable physical arguments, but did not give formal derivations from QCD.

The presence of the quark momenta $\mathbf{p}_i$ in the Thomas-type spin-dependent interactions in Eq. (2.2) suggests that new contributions to the magnetic moment operator could arise in a complete theory through the minimal substitution

$$\mathbf{p}_i \to \mathbf{p}_i - e_i \mathbf{A}_{\rm em}(x_i), \tag{2.3}$$

with $\mathbf{A}_{\rm em}(x_i)$ the electromagnetic vector potential associated with an external magnetic field. We have therefore redone the calculation of Brambilla *et al.* with the gauge interaction

TABLE I. The values in GeV of the matrix elements ϵ and Σ defined in Eqs. (2.9) and (2.10). The matrix elements were evaluated for $\alpha_s=0.39$, $\sigma=0.18$ GeV^2, $m_u=m_d=0.343$ GeV, and $m_s=0.539$ GeV.

Baryon	ϵ	ϵ'	$\tilde{\epsilon}$	Σ	Σ'	$\tilde{\Sigma}$
N	0.014	0.014	0.014	0.062	0.062	0.062
Σ	0.014	0.018	0.012	0.061	0.069	0.046
Ξ	0.016	0.012	0.018	0.053	0.046	0.068
Ω	0.016	0.016	0.016	0.052	0.052	0.052

extended to include $A_{\rm em}$. After reorganizing the calculation to keep the presence of $A_{\rm em}$ explicit throughout, and then expanding to first order in $e_q A_{\rm em}$ in the baryon rest frame with

$$\mathbf{A}_{\rm em}=\tfrac{1}{2}\mathbf{B}\times\mathbf{x}_q\,,\quad \mathbf{B}=\text{const}, \tag{2.4}$$

we can identify the modified magnetic moment operator through the relation

$$\Delta H=-\boldsymbol{\mu}\cdot\mathbf{B}. \tag{2.5}$$

The new moment operator, $\boldsymbol{\mu}=\boldsymbol{\mu}^{(\rm QM)}+\Delta\boldsymbol{\mu}^{QM}$, involves the leading corrections to the quark-model operator associated with the binding interactions. $\Delta\boldsymbol{\mu}$ *can*, in fact, be read off from the terms in Eq. (2.2) which depend on both the quark spins and momenta by making the minimal substitution in Eq. (2.3). For example, the term which depends on $\mathbf{s}_1\cdot\mathbf{r}_{12}\times\mathbf{p}_1$ gives an extra contribution

$$\frac{e_1}{6m_1^2}\mathbf{x}_1\times(\mathbf{s}_1\times\mathbf{r}_{12})\,\frac{\alpha \mathrm{s}}{r_{12}^3} \tag{2.6}$$

to $\boldsymbol{\mu}_1$. There are also possible orbital contributions to the moments because the Hamiltonian mixes states with nonzero orbital angular momenta with the ground state. These contributions proved to be negligible [1].

The moment of a baryon b is now given by

$$\mu_b=\sum_q\,(\mu_q+\Delta\mu_q^b)\langle\sigma_{q,z}\rangle_b=\mu_b^{QM}+\sum_q\,\Delta\mu_q^b\langle\sigma_{q,z}\rangle_b\,, \tag{2.7}$$

where the sum is over the quarks in the baryon and we have quantized along **B**, taken along the z axis. The spin expectation values are to be calculated in the baryon ground state.

Note that the correction $\Delta\mu_q^b$ to the moment of quark q depends on the baryon b in which it appears. The final baryon moments depart from the quark model pattern only when the ratios $\Delta\mu_q^b/\mu_q$ differ in different baryons.

B. Results for the octet baryons

The general result for the moment operator given above can be simplified considerably for the $L=0$ ground state baryons. The absence of any orbital angular momentum allows us to integrate immediately over angles. Furthermore, two quarks always have the same mass in each octet or decuplet baryon, so appear symmetrically in the spatial part of a flavor-independent wave function. We will label these quarks 1 and 2, let $m_1=m_2=m$, and take 3 as the odd-mass quark if there is one. With this labeling, the spatial matrix elements of the new operators can be reduced to a small set, and the correction terms become

$$\begin{aligned}
\Delta\mu_1^b&=\mu_1\left[\frac{\epsilon+\epsilon'}{2m}+\frac{1}{e_1}\left(\frac{e_2}{m}\epsilon+\frac{e_3}{m_3}\tilde{\epsilon}\right)-\frac{\Sigma+\Sigma'}{2m}\right],\\
\Delta\mu_2^b&=\mu_2\left[\frac{\epsilon+\epsilon'}{2m}+\frac{1}{e_2}\left(\frac{e_1}{m}\epsilon+\frac{e_3}{m_3}\tilde{\epsilon}\right)-\frac{\Sigma+\Sigma'}{2m}\right],\\
\Delta\mu_3^b&=\mu_3\left[\frac{\tilde{\epsilon}}{m_3}+\frac{1}{e_3}\,\frac{e_1+e_2}{m}\epsilon'-\frac{\tilde{\Sigma}}{m_3}\right],
\end{aligned} \tag{2.8}$$

where the ϵ's and Σ's are ground state radial matrix elements,

$$\begin{aligned}
\epsilon&=\left\langle\frac{2\alpha_s}{9}\,\frac{\mathbf{r}_{12}\cdot\mathbf{x}_1}{r_{12}^3}\right\rangle_b=\left\langle\frac{\alpha_s}{9}\,\frac{1}{r_{12}}\right\rangle_b,\\
\epsilon'&=\left\langle\frac{2\alpha_s}{9}\,\frac{\mathbf{r}_{23}\cdot\mathbf{x}_2}{r_{23}^3}\right\rangle_b=\left\langle\frac{2\alpha_s}{9}\,\frac{\mathbf{r}_{13}\cdot\mathbf{x}_1}{r_{31}^3}\right\rangle_b,\\
\tilde{\epsilon}&=\left\langle\frac{2\alpha_s}{9}\,\frac{\mathbf{r}_{31}\cdot\mathbf{x}_3}{r_{31}^3}\right\rangle_b=\left\langle\frac{2\alpha_s}{9}\,\frac{\mathbf{r}_{32}\cdot\mathbf{x}_3}{r_{23}^3}\right\rangle_b,
\end{aligned} \tag{2.9}$$

and

$$\begin{aligned}
\Sigma&=\frac{\sigma}{6}\left\langle\frac{\mathbf{r}_{12}\cdot\mathbf{x}_1}{r_{12}}\right\rangle_b=\frac{\sigma}{12}\langle r_{12}\rangle_b\,,\\
\Sigma'&=\frac{\sigma}{6}\left\langle\frac{\mathbf{r}_{23}\cdot\mathbf{x}_2}{r_{23}}\right\rangle_b=\frac{\sigma}{6}\left\langle\frac{\mathbf{r}_{31}\cdot\mathbf{x}_1}{r_{31}}\right\rangle_b,\\
\tilde{\Sigma}&=\frac{\sigma}{6}\left\langle\frac{\mathbf{r}_{31}\cdot\mathbf{x}_3}{r_{31}}\right\rangle_b=\frac{\sigma}{6}\left\langle\frac{\mathbf{r}_{32}\cdot\mathbf{x}_3}{r_{23}}\right\rangle_b.
\end{aligned} \tag{2.10}$$

In writing these results, we have made the approximation $r_1+r_2+r_3\approx\frac{1}{2}(r_{12}+r_{23}+r_{31})$, known to be reasonably accurate for the ground state baryons [12], and used the corresponding Thomas spin interaction.

We have evaluated the the radial matrix elements above using Gaussian wave functions obtained in a variational calculation of the ground state energies for the Hamiltonian in

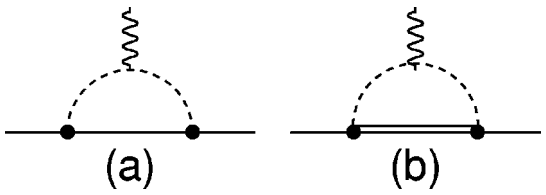

FIG. 2. Diagrams with couplings independent of the baryon moments. These diagrams lead to the non-analytic $m_s^{1/2}$ corrections to the baryon magnetic moments in the conventional ChPT. The dashed lines denote the mesons, the single and double solid lines denote octet and decuplet baryons, respectively. A heavy dot with a meson line represents a form factor $F(k,v)$ [Eq. (3.14)], where k is the meson momentum.

Eq. (2.2). The results are given in Table I for $\alpha_s=0.39$ and $\sigma=0.18$ GeV^2, values taken from fits to the baryon spectrum [12,13] using the same Hamiltonian. A refitting of the octet moments using μ_u and μ_s as adjustable parameters in the QM contribution to the complete expression in Eq. (2.7) gives only a slight improvement in the results, with an incorrect pattern in the corrections relative to those needed.

III. LOOP CORRECTIONS TO THE MOMENTS

Given the failure of the binding corrections to eliminate the deficiencies in the QCD-based quark model, we have reexamined the approximations used in its derivation [1]. A key element in the Wilson-loop construction was the use of the quenched approximation in which all internal quark loops are omitted. As discussed elsewhere [1], it appears that this approximation is the one most likely to account for the difficulty in reproducing the measured moments. In particular, the introduction of quark loops allows meson loops to appear, and these are known to affect magnetic moments. The first step in the improvement of the model is therefore the introduction of meson loop corrections to the QM moments. The relevant one-loop Feynman diagrams at the hadronic level are shown in Figs. 2 and 3. Since the ground state $L=0$ octet and decuplet baryons only differ in their internal spin configurations in the simple QM and the octet-decuplet mass differences are small, we must include both sets of baryon states in the calculation to get a consistent theory. However, we include only the pseudoscalar mesons.

The diagrams in Fig. 2 are independent of the input magnetic moments of the baryons, but modify the final moments. In contrast, the diagrams in Fig. 3 involve the octet and decuplet moments and the octet-decuplet transition moment directly. We will specify these in terms of the QM.

We will calculate the contributions of the diagrams in Figs. 2 and 3 using heavy baryon perturbation theory (HBPT) in which the baryon masses are assumed to be large compared to the typical scale set by the internal momenta. It will be essential in this respect to take the extended, composite structure of the baryons into account, since this extended structure naturally limits the momenta that can be absorbed by the baryon as a whole. The resulting momenta are small on the average, well below usual chiral cutoff at ≈ 1 GeV, and it is therefore reasonable to use the lowest

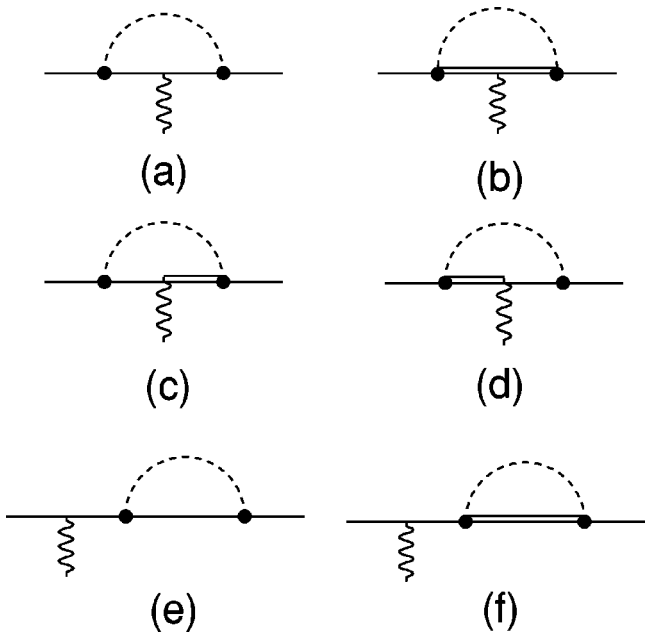

FIG. 3. Diagrams with couplings that depend on the tree-level baryon moments. These diagrams lead to non-analytic $m_s \ln m_s$ corrections to the baryon magnetic moments in the conventional ChPT.

order chiral couplings to describe the resulting low momentum, long distance interactions of the mesons and baryons.[1] We will discuss these ingredients separately in the following subsections.

A. Heavy baryon couplings

Heavy baryon perturbation theory was developed in Ref. [9] and extended to the chiral context in Ref. [10]. It has been used to study a number of hadronic processes at momentum transfers much less than 1 GeV. The key ideas in HBPT involve the replacement of the momentum p^μ of a nearly on-shell baryon by its on-shell momentum $m_B v^\mu$ plus a small additional momentum k^μ, $p=m_B v+k$, and the replacement of the baryon field operator $B(x)$ by an operator $B_v(x)$ constructed to remove the free momentum dependence in the Dirac equation,

$$B_v(x)=e^{im_B \not{v} v^\mu x_\mu} B(x). \tag{3.1}$$

In these expressions v^μ is the on-shell four velocity of the

[1]The difficulties with ChPT in the present context result from the treatment of the baryons and mesons as point particles in HBChPT. This leads to divergences in loop integrals. Different regularization schemes lead to different results for the integrals, for example, in dimensional [14] and momentum [15] regularization, with the ambiguities being lumped into the new couplings that must be introduced along with the loop diagrams. The present theory has a natural cutoff at fairly low momentum imposed by the extended structure of the hadrons in the QM, and the loop contributions are finite. However, they change the initial structure of the theory, and provide in effect a dynamical calculation of what would appear as new couplings in ChPT.

baryon and it is assumed that $k\cdot v \ll m_B$. The perturbation expansion then involves modified Feynman rules and an expansion in powers of k/m_B. We will work to leading order in this expansion.

The low-momentum couplings of mesons to baryons appear to be well described as derivative couplings with the standard chiral structure. We will use these couplings in our analysis, but emphasize that we are not doing the usual momentum expansion of ChPT in the sense that the higher-order effective couplings of ChPT will be implicit output of our dynamical calculation. The Lagrangian for the modified baryon fields depends on the usual matrix of baryon fields, with B replaced by B_v, and on the pseudoscalar pion octet normalized as

$$\boldsymbol{\phi}=\frac{1}{\sqrt{2}}\begin{pmatrix} \frac{\pi^0}{\sqrt{2}}+\frac{\eta}{\sqrt{6}} & \pi^+ & K^+ \\ \pi^- & -\frac{\pi^0}{\sqrt{2}}+\frac{\eta}{\sqrt{6}} & K^0 \\ K^- & \bar{K}^0 & -\frac{2\eta}{\sqrt{6}} \end{pmatrix}. \quad (3.2)$$

This couples to the baryon fields at low momenta through the vector and axial vector currents defined by

$$V_\mu=f^{-2}(\phi\partial_\mu\phi-\partial_\mu\phi\phi)+\cdots, \quad A_\mu=f^{-1}\partial_\mu\phi+\cdots, \quad (3.3)$$

where $f\approx 93$ MeV is the meson decay constant. We will retain, as indicated above, only leading term in the derivative expansion. The Lagrangian for octet and decuplet baryons is then

$$\begin{aligned}\mathcal{L}_v=&\, i\ \mathrm{Tr}\ \bar{B}_v(v\cdot\mathcal{D})B_v+2D\ \mathrm{Tr}\ \bar{B}_vS_v^\mu\{A_\mu,B_v\}\\ &+2F\ \mathrm{Tr}\ \bar{B}_vS_v^\mu[A_\mu,B_v]-i\bar{T}_v^\mu(v\cdot\mathcal{D})T_{v\mu}+\delta\bar{T}_v^\mu T_{v\mu}\\ &+\mathcal{C}(\bar{T}_v^\mu A_\mu B_v+\bar{B}_vA_\mu T_v^\mu)+2\mathcal{H}\bar{T}_v^\mu S_{vv}A^\nu T_{v\mu}\\ &+\mathrm{Tr}\ \partial_\mu\phi\partial^\mu\phi+\cdots \end{aligned} \quad (3.4)$$

where δ is the decuplet-octet mass difference, and $\mathcal{D}_\mu=\partial_\mu+[V_\mu,]$ is the covariant chiral derivative. B_v is now the matrix of octet baryon fields, and the Rarita-Schwinger fields T_v^μ [10] represent the decuplet baryons. D, F, $\mathcal{C}$, and $\mathcal{H}$ are the strong interaction coupling constants. The spin operator S_v^μ is defined in Ref. [10].

The electromagnetic interactions of the mesons, and the convection current interactions of the baryons, are introduced into the Lagrangian by making the substitutions

$$\begin{aligned}&\mathcal{D}_\mu\to\mathcal{D}_\mu+ie\mathcal{A}_\mu[Q,],\\ &\partial_\mu\phi\to\mathcal{D}_\mu\phi=\partial_\mu\phi+ie\mathcal{A}_\mu[Q,\phi],\end{aligned} \quad (3.5)$$

where $\mathcal{A}_\mu$ is the photon field. The baryon moment couplings needed in the graphs in Fig. 3 do not appear above and require a separate treatment.

B. Quark model moment couplings

As described above, our starting point for calculating the baryon moments is the QCD-based quark model. These moments play the role of tree-level interactions in the loop expansion and also appear in the electromagnetic interactions of the internal baryons in Fig. 3. As we noted in [7], the octet baryon moments can be written in terms of the general SU(3) symmetry breaking operator in HBChPT given by [2–6],

$$\mathcal{L}_{SB}=\mathcal{L}_0+\mathcal{L}_1 \quad (3.6)$$

where

$$\begin{aligned}\mathcal{L}_0=&\frac{e}{4m_N}(\mu_D\mathrm{Tr}\ \bar{B}_vF_{\mu\nu}\sigma^{\mu\nu}\{Q,B_v\}\\ &+\mu_F\mathrm{Tr}\ \bar{B}_vF_{\mu\nu}\sigma^{\mu\nu}[Q,B_v]),\end{aligned} \quad (3.7)$$

is the leading order moment operator in chiral perturbation theory parametrized by μ_D and μ_F [8], and

$$\begin{aligned}\mathcal{L}_1=&\frac{e}{4m_N}F_{\mu\nu}(c_1\mathrm{Tr}\ \bar{B}_v\mathcal{M}Q\sigma^{\mu\nu}B_v+c_2\mathrm{Tr}\bar{B}_vQ\sigma^{\mu\nu}B_v\mathcal{M}\\ &+c_3\mathrm{Tr}\ \bar{B}_v\sigma^{\mu\nu}B_v\mathcal{M}Q+c_4\mathrm{Tr}\ \bar{B}_v\mathcal{M}\sigma^{\mu\nu}B_vQ\\ &+c_5\mathrm{Tr}\ \bar{B}_v\sigma^{\mu\nu}B_v\mathrm{Tr}\ \mathcal{M}Q)\end{aligned} \quad (3.8)$$

contains the new couplings $c_1,\ldots,c_5$ introduced along with the counterterms that are necessary at one loop [2–6]. Here $Q=\mathrm{diag}(2/3,-1/3,-1/3)$ is the quark charge matrix and $\mathcal{M}=\mathrm{diag}(0,0,1)$ is proportional to the mass matrix used to introduce SU(3) breaking through the strange-quark mass m_s. The addition to $\mathcal{L}_{SB}$ of one further coupling which is second order in m_s,[2]

$$\mathcal{L}_2=\frac{ed}{4m_N}\mathrm{Tr}\ \bar{B}_v\mathcal{M}Q\sigma^{\mu\nu}F_{\mu\nu}B_v\mathcal{M} \quad (3.9)$$

gives a complete basis for the description of the octet moments [7].

The particular choice $\mu_F=2\mu_D/3=\mu_u$ and $c_1=-5\Delta$, $c_2=0$, $c_3=-\Delta$, $c_4=0$, and $c_5=\Delta$, $d=0$ for the parameters above, with $\Delta=(2\mu_s+\mu_u)/2$, gives us the QM octet moments

$$\mu_p^{(QM)}=\frac{3}{2}\mu_u, \quad \mu_{\Sigma^+}^{(QM)}=\frac{4}{3}\mu_u-\frac{1}{3}\mu_s, \quad (3.10)$$

[2]Since $\mathcal{M}Q=Q\mathcal{M}=-\frac{1}{3}\mathcal{M}$, the rearrangements of the factors $\mathcal{M}$Q and $\mathcal{M}$ in Eq. (3.9) give no new contributions to $\mathcal{L}_2$, and the form given is the only new invariant.

$$\mu_{\Xi^0}^{(QM)}=\frac{4}{3}\mu_s-\frac{1}{3}\mu_u,$$

$$\mu_n^{(QM)}=-\mu_u,\quad \mu_{\Sigma^0}^{(QM)}=\frac{1}{3}(\mu_u-\mu_s),$$

$$\mu_{\Xi^-}^{(QM)}=\frac{1}{6}\mu_u+\frac{4}{3}\mu_s,\quad \mu_\Lambda^{(QM)}=\mu_s,$$

$$\mu_{\Sigma^-}^{(QM)}=-\frac{2}{3}\mu_u-\frac{1}{3}\mu_s,$$

$$\mu_{\Lambda\Sigma^0}^{(QM)}=\frac{\sqrt{3}}{2}\mu_u.$$

Since the one loop corrections involve both intermediate octet and decuplet baryon states, we also need the Lagrangians for the QM decuplet magnetic moment couplings and the QM octet-decuplet transition magnetic moment couplings. These are given, respectively, by

$$\mathcal{L}^{(3/2)}=-i\frac{3e}{2m_N}\overline{T}^{\mu}_{vikl}\hat{Q}^i_j T_v^{\nu jkl}F_{\mu\nu}, \tag{3.11}$$

and

$$\mathcal{L}^{(od)}=-i\frac{2e}{m_N}F_{\mu\nu}(\epsilon_{ijk}\hat{Q}^i_l\overline{B}^j_{vm}S^\mu_v T_v^{\nu klm}+\text{H.c.}), \tag{3.12}$$

where i, j, k, l, and m are SU(3) flavor indices and $\hat{Q}=\text{diag}(\mu_u,-\mu_u/2,\mu_s)$.

C. Meson wave function effects: The form factor

The baryons in the QM are composite states, and can absorb only limited recoil momentum, while remaining in their ground states. This must be taken into account in a dynamical model. In the absence of a detailed theory of the interactions of composite mesons and baryons, we will model the wave function effects using a form factor at each meson-baryon vertex. In keeping with the heavy baryon picture, we will define the form factor in the rest frame of the baryon where it can depend only on $\mathbf{k}^2$, the square of the three momentum of the meson. A form factor of this type automatically respects crossing, since a change $\mathbf{k}\to-\mathbf{k}$ corresponding to a shift of a meson between the initial and final states does not change the form factor.

We have chosen for simplicity to use an one-parameter form factor

$$F(\mathbf{k})=\frac{\lambda^2}{\lambda^2+\mathbf{k}^2} \tag{3.13}$$

normalized at chiral limit, $\mathbf{k}=0$. The parameter λ characterizes the natural momentum scale, expected to be much below 1 GeV. With the introduction of this form factor, all the diagrams in Figs. 2 and 3 are finite and no arbitrary subtractions need to be introduced into the theory.

The evaluation of momentum integrals in the presence of the form factor is straightforward, but involves some new elements. First, the form factor (3.13) is rewritten in covariant form as

$$F(k,v)=\frac{-\lambda^2}{k^2-(k\cdot v)^2-\lambda^2}. \tag{3.14}$$

The factors in the denominator of a one-loop integrand with integration variable k can be combined using the Feynman parametrization formula to obtain an expression of the form

$$k^2+\alpha(k\cdot v)^2+\beta(k\cdot v)+\gamma. \tag{3.15}$$

Here α, β, and γ are quantities independent of the loop momentum k, and the photon momentum q has been set equal to zero in the denominators. A change of the variable of integration to

$$k'=k+(\pm\sqrt{1+\alpha}-1)v(k\cdot v) \tag{3.16}$$

then brings Eq. (3.15) to the standard form

$$k'^2\pm\frac{\beta}{\sqrt{1+\alpha}}(k'\cdot v)+\gamma, \tag{3.17}$$

and the loop integral is easily evaluated. Note that the Jacobian of the transformation of variables in Eq. (3.16) is $1/\sqrt{1+\alpha}$.

IV. BARYON MAGNETIC MOMENTS

A. Expressions for the octet baryon moments

We can now give our expressions for the baryon magnetic moments including the loop corrections from the diagrams shown in Figs. 2 and 3. In units of nuclear magnetons, the moment of baryon i is

$$\mu_i=\mu_i^{(0)}+\mu_i^{(1/2)}+\mu_i^{(3/2)}, \tag{4.1}$$

where the leading term $\mu_i^{(0)}$ includes the QM moments plus the corrections $\Delta\mu_i^{QM}$ obtained in the QCD-based QM, while $\mu_i^{(1/2)}$ and $\mu_i^{(3/2)}$ are the contributions from the one-loop graphs with intermediate octet and decuplet baryon states, respectively. We find that

$$\mu_i^{(0)}=\alpha_i+\Delta\mu_i^{QM}, \tag{4.2}$$

$$\mu_i^{(1/2)}=\sum_{X=\pi,K}-\frac{m_N}{24\pi f^2}\frac{\lambda^4}{(\lambda+m_X)^3}\beta_i^{(X)} + \sum_{X=\pi,K,\eta}\frac{1}{16\pi^2 f^2}(\gamma_i^{1(X)}-2\lambda_i^{(X)}\alpha_i)L_0(m_X,\lambda), \tag{4.3}$$

and

$$\mu_i^{(3/2)} = \sum_{X=\pi,K} \frac{m_N}{8\pi f^2} \tilde{F}(m_X,\delta,\lambda)\tilde{\beta}_i^{(X)} + \sum_{X=\pi,K,\eta} \frac{1}{32\pi^2 f^2} \times [(\tilde{\gamma}_i^{1(X)} - 2\tilde{\lambda}_i^{(X)}\alpha_i)L_1(m_X,\delta,\lambda) + \tilde{\gamma}_i^{2(X)} L_2(m_X,\delta,\lambda)], \quad (4.4)$$

where $\alpha_i = \mu_i^{(QM)}$. The coupling coefficients $\beta_i^{(X)}$, $\tilde{\beta}_i^{(X)}$, $\lambda_i^{(X)} + \tilde{\lambda}_i^{(X)}$ are identical to those in Ref. [2], and will not be given here.[3] The remaining coefficients $\gamma_i^{1(X)}$, $\tilde{\gamma}_i^{1(X)}$, and $\tilde{\gamma}_i^{2(X)}$ depend explicitly on μ_u and μ_s, and have not appeared elsewhere. We list those coefficients in Appendix A.

To connect the various terms to the loop graphs in Figs. 2 and 3, we note that $\beta_i^{(X)}$, $\tilde{\beta}_i^{(X)}$, $\gamma_i^{1(X)}$, $\tilde{\gamma}_i^{1(X)}$, $\tilde{\gamma}_i^{2(X)}$, $\lambda_i^{(X)}$, and $\tilde{\lambda}_i^{(X)}$ are the coefficients of the graphs 2a, 2b, 3a, 3b, 3c (or 3d), 3e and 3f, respectively.

The expressions for the functions $L_0(m_X,\lambda)$, $\tilde{F}(m_X,\delta,\lambda)$, $L_1(m_X,\delta,\lambda)$, and $L_2(m_X,\delta,\lambda)$ are given in Appendix B. These functions result from the loop integrations, and depend on the meson masses, the decuplet-octet mass difference δ, and the natural wave function cutoff λ. We emphasize that the loop integrations are all finite, and that the wave function parameter λ sets the natural momentum scale in graphs that are divergent for point particles.

B. Fits to the data

We have used the foregoing expressions to fit the experimental baryon magnetic moments. It is worth emphasizing that all the parameters that appear except for μ_u, μ_s, and λ are known independently. We evaluated the corrections $\Delta\mu_i^{QM}$ given in Eqs. (2.7) and (2.8) from the QCD-based QM using the matrix elements given in Table I and quark masses $m_u = m_d = 0.343$ GeV and $m_s = 0.539$ GeV chosen to give the best fit to the octet magnetic moments in the naive QM. The strong interaction couplings F, D, and $\mathcal{C}$ were chosen to satisfy the SU(6) relations $F = 2D/3$, $\mathcal{C} = -2D$ expected in the QM, with the values $F = 0.5$, $D = 0.75$, and $\mathcal{C} = -1.5$ chosen so that $F + D \approx |g_A/g_V| = 1.26$. The decuplet coupling $\mathcal{H}$ does not appear. The decuplet-octet mass difference was taken as $\delta = 250$ MeV; the results are fairly insensitive to this choice. Finally, we used the values $f_\pi = 93$ MeV and $f_K = f_\eta = 1.2 f_\pi$ [2].

The results of an equal weight least square fit to the seven well-measured octet moments using the three free parameters μ_u, μ_s, and λ are summarized in Table II. We find root-mean-square deviation of the predicted values from the observation of 0.055 μ_N. This is a substantial improvement on the naive quark model which gives an average deviation of 0.12 μ_N. The transition moment $\mu_{\Sigma^0\Lambda}$ was not included in the fit, but was left as a prediction. The result obtained, $\mu_{\Sigma^0\Lambda} = 1.559\,\mu_N$, differs from the experimental value $\mu_{\Sigma^0\Lambda} = 1.610 \pm 0.08\ \mu_N$, by 0.05 μ_N, a value within the experimental uncertainty and one that does not affect the overall fit.

TABLE II. The magnetic moments from the naive quark model (QM) and the QCD-based QM with loop corrections. The root-mean-square deviations from experimental values are about 0.11 and 0.05 for the QM and the QCD-based QM with loop corrections, respectively. All moments and deviations are given in units of μ_N.

μ_B	QM	QCD QM+loops	Experiment
p	2.728	2.720	2.793 ± 0.000
n	-1.818	-1.946	-1.913 ± 0.000
Σ^+	2.618	2.519	2.458 ± 0.010
Σ^-	-1.019	-1.110	-1.160 ± 0.025
Σ^0	0.800	0.705	–
Λ	-0.580	-0.608	-0.613 ± 0.004
Ξ^0	-1.380	-1.316	-1.250 ± 0.014
Ξ^-	-0.470	-0.582	-0.651 ± 0.003
$\Sigma^0\Lambda$	1.575	1.559	$\pm 1.610 \pm 0.08$
μ_u	1.818	2.083	–
μ_s	-0.580	-0.656	–
λ (in MeV)	–	407	–

A detailed breakdown of the contributions of the loop integrals to the fitted magnetic moments of the octet baryons is given in Table III. The results in this table shows that the loop contributions are small in comparison to the leading QM contributions, suggesting reasonably rapid convergence of the loop expansion. This is in marked contrast to the results obtained in HBChPT, where the loop contributions calculated using dimensional regularization are comparable in size to the leading terms in the chiral expansion [7]. It is also clear from the table that the binding corrections $\Delta\mu_i^{QM}$ found in the QCD-based derivation of the QM [1] are important. It is not possible to obtain as good a fit to the data as given in Table II when these are omitted.

A further interesting point involves the importance of the decuplet intermediate states for the octet moments. It is easy to check that the contributions from the graphs involving decuplet states, that is, the sum of the contributions from the graphs 2b, 3b, 3c, 3d, and 3f, are substantial. For most of the baryons, those contributions are larger than those from the graphs which involve only the intermediate octet states. This result is insensitive to the value used for the octet-decuplet mass difference. We conclude that the decuplet must be regarded as a set of light baryon states as in the QM, and not, as in [5] as a set of heavy states. The present method for obtaining the loop corrections to the QM moments should therefore apply to the decuplet moments as well. That calculation has been carried out elsewhere [16] using the same values of μ_u, μ_s, and λ as obtained here, and gives a pre-

[3]The tadpole graph 2b in Ref. [2] is absent in our model. Since the chiral symmetry is broken in the QM, we do not include chiral corrections to the baryon moment operators as in that reference. The elementary $\bar{B}B\phi\phi\mathcal{A}_\mu$ vertex connected with spin operator therefore does not appear, but the inclusion of higher mass baryons in the intermediate states would lead to effective vertex with this structure.

TABLE III. Detailed breakdown of the contributions of the loop integrals to the fitted magnetic moments of the octet baryons (in μ_N). Those contributions are evaluated at $F=0.5$, $D=0.75$, $\mathcal{C}=-1.5$. As shown in Table I, a best fit is obtained at $\mu_u=2.083$, $\mu_s=-0.656$ and the natural cutoff $\lambda=407$ MeV. $\Delta\mu_B$ stands for a deviation from the experimently measured value. The superscripts (N) and (Δ) are used to indicate that the intermediate baryon states are octet and decuplet, respectively.

μ_B	μ_u, μ_s	$\tilde{\Delta}\mu_i$	$m_s^{1/2(N)}$	$\ln m_s^{(N)}$	$m_s^{1/2(\Delta)}$	$\ln m_s^{(\Delta)}$	Loops	μ_B	$\Delta\mu_B$
p	3.124	−0.500	0.416	−0.729	0.057	0.353	0.096	2.720	−0.072
n	−2.083	0.427	−0.381	0.409	−0.067	−0.253	−0.291	−1.946	−0.033
Σ^+	2.995	−0.428	0.273	−0.536	−0.002	0.217	−0.048	2.519	0.061
Σ^-	−1.170	0.139	−0.217	0.188	0.021	−0.072	−0.080	−1.110	0.050
Σ^0	0.913	−0.145	0.028	−0.174	0.010	0.073	−0.064	0.705	
Λ	−0.656	0.085	−0.028	0.073	−0.010	−0.073	−0.037	−0.608	0.005
Ξ^0	−1.569	0.271	−0.043	0.128	−0.043	−0.059	−0.017	−1.316	−0.066
Ξ^-	−0.528	−0.056	−0.048	0.061	0.033	−0.044	0.002	−0.582	0.069
$\Sigma^0\Lambda$	1.804	−0.378	0.229	−0.268	0.058	0.114	0.134	1.559	−0.051

diction $\mu_{\Omega^-}=-1.97\ \mu_N$ in striking agreement with the measured value $-2.02\pm0.05\ \mu_N$, and much better than the prediction of the naive QM, $\mu_{\Omega^-}=-1.74\ \mu_N$.

C. Conclusions and prospects

In this paper, we have considered the one-loop corrections to the octet baryon magnetic moments in the QCD-based QM. It is necessary to include these as a first step in getting away from the quenching of internal quark loops used in the derivation of the QM.

Our approach to the calculation is based on HBPT. We use the derivative couplings for the low-momentum interactions of the pseudoscalar mesons with the baryons favored by ChPT, and a form factor to characterize the composite structure of baryons. The loop diagrams are all finite, and no counterterms need to be introduced to absorb divergences. We are, in fact, making a dynamical calculation of the extra couplings or counterterms encountered in HBChPT in the sense that our expressions for the eight octet moments can be parametrized exactly [7] in terms of the eight chiral couplings defined in Eqs. (3.7), (3.8) and (3.9).

The results from our fits to the octet baryon moments using the QCD-based QM with loop corrections are very good, with an average deviation of the theoretical moments from theory of $0.05\ \mu_N$, significantly better than the QM results. The contribution from each loop graph is small compared to the leading terms, suggesting convergence of the loop expansion. The parameter λ which sets the momentum scale in the meson-baryon interaction or wave function is about 400 MeV, a value consistent with the expectations deduced from the observed transverse momentum distributions in pion production. This value is closer to the kaon mass than to the pion mass. As a result, the wave function effects suppress the short-distance contributions from kaon and η-loops, but affect the more reliable long-distance part of the pion loop contributions relatively little. We conclude that it is crucial to take the effects of compositeness into account if one is to have a controllable perturbation theory for hadrons at low momentum.

A question which arises at this point concerns the extent to which the theory can be further improved by the inclusion of higher-mass mesons and baryons. The contributions of the ground state vector mesons would be expected to be as important as the contributions from the pseudoscalar mesons except for the suppression of high mass intermediate states by the momentum cutoff imposed by the wave functions. The contributions of higher mass baryons in the intermediate states are also suppressed. However, there are low-mass multiparticle intermediate states such as those with one baryon and two pions that could be important. A possible approach to the estimation of their effects is through the use of the sideways or mass dispersion relations proved by Bincer [17].

We remark, finally, that we believe that this work demonstrates the importance of getting beyond the quenched approximation in lattice QCD if one is to understand the finer details of hadron structure from first principles.

ACKNOWLEDGMENTS

This work was supported in part by the U.S. Department of Energy under Grant No. DE-FG02-95ER40896. One of the authors (L.D.) would like to thank the Aspen Center for Physics for its hospitality, while parts of this work were done.

APPENDIX A: THE COUPLING COEFFICIENTS

In this appendix, the coupling coefficients are explained and presented explicitly. For simplicity, the superscript (X) is suppressed. Our β_i, and $\tilde{\beta}_i$ are identical, respectively, to the coefficients β_i and β_i' in Ref. [2]. The sum of our coefficients λ_i and $\tilde{\lambda}_i$ is equal to the coefficient $\overline{\lambda_i}$ defined in [2]:

$$\lambda_i+\tilde{\lambda}_i=\overline{\lambda_i}. \tag{A1}$$

Since the couplings associated with graphs which involve only octet intermediate states are independent of those for graphs which involve decuplet intermediate states, it is easy to separate λ_i and $\tilde{\lambda}_i$ from the combined coefficient given in [2].

The values of the coupling factors γ_i^1 evaluated from the graphs in Fig. 3(a) are

$$\gamma_p^{1(\pi)}=\frac{1}{4}(D+F)^2\mu_u,$$

$$\gamma_n^{1(\pi)}=-(D+F)^2\mu_u,$$

$$\gamma_\Lambda^{1(\pi)}=\frac{2}{3}D^2(\mu_s-\mu_u),$$

$$\gamma_{\Sigma^+}^{1(\pi)}=\frac{2}{3}[(3DF-5F^2)\mu_u+(2F^2-D^2)\mu_s],$$

$$\gamma_{\Sigma^0}^{1(\pi)}=\frac{2}{3}[-2F^2\mu_u+(2F^2-D^2)\mu_s],$$

$$\gamma_{\Sigma^-}^{1(\pi)}=\frac{2}{3}[(-3DF+F^2)\mu_u+(2F^2-D^2)\mu_s],$$

$$\gamma_{\Xi^0}^{1(\pi)}=-2(F-D)^2\mu_s,$$

$$\gamma_{\Xi^-}^{1(\pi)}=\frac{1}{4}(F-D)^2(\mu_u-8\mu_s),$$

$$\gamma_{\Lambda\Sigma^0}^{1(\pi)}=\frac{1}{\sqrt{3}}D(4F-D)\mu_u, \tag{A2}$$

for the pion loops,

$$\gamma_p^{1(K)}=(F-D)(D-3F)\mu_u+\left(\frac{1}{3}D^2-2DF-F^2\right)\mu_s,$$

$$\gamma_n^{1(K)}=2F(F-D)\mu_u+\left(\frac{1}{3}D^2-2DF-F^2\right)\mu_s,$$

$$\gamma_\Lambda^{1(K)}=-\frac{1}{18}(D^2+12DF+9F^2)\mu_u-\frac{4}{9}(D-3F)^2\mu_s,$$

$$\gamma_{\Sigma^+}^{1(K)}=-\frac{7}{6}\left(D^2-\frac{22}{7}DF+F^2\right)\mu_u-\frac{4}{3}(D+F)^2\mu_s,$$

$$\gamma_{\Sigma^0}^{1(K)}=-\frac{1}{6}(D^2-4DF+F^2)\mu_u-\frac{4}{3}(D+F)^2\mu_s,$$

$$\gamma_{\Sigma^-}^{1(K)}=\frac{5}{6}\left(D^2-\frac{14}{5}DF+F^2\right)\mu_u-\frac{4}{3}(D+F)^2\mu_s,$$

$$\gamma_{\Xi^0}^{1(K)}=-2D(D+F)\mu_u+\frac{1}{3}(D^2+6DF-3F^2)\mu_s,$$

$$\gamma_{\Xi^-}^{1(K)}=(D^2-F^2)\mu_u+\frac{1}{3}(D^2+6DF-3F^2)\mu_s,$$

$$\gamma_{\Lambda\Sigma^0}^{1(K)}=\frac{1}{2\sqrt{3}}(3D^2+4DF-9F^2)\mu_u \tag{A3}$$

for the kaon loops, and

$$\gamma_p^{1(\eta)}=-\frac{1}{4}(3F-D)^2\mu_u,$$

$$\gamma_n^{1(\eta)}=\frac{1}{6}(3F-D)^2\mu_u,$$

$$\gamma_\Lambda^{1(\eta)}=-\frac{2}{3}D^2\mu_s,$$

$$\gamma_{\Sigma^+}^{1(\eta)}=-\frac{2}{9}D^2(4\mu_u-\mu_s),$$

$$\gamma_{\Sigma^0}^{1(\eta)}=-\frac{2}{9}D^2(\mu_u-\mu_s),$$

$$\gamma_{\Sigma^-}^{1(\eta)}=\frac{2}{9}D^2(2\mu_u+\mu_s),$$

$$\gamma_{\Xi^0}^{1(\eta)}=\frac{1}{18}(D+3F)^2(\mu_u-4\mu_s),$$

$$\gamma_{\Xi^-}^{1(\eta)}=-\frac{1}{36}(D+3F)^2(\mu_u+8\mu_s),$$

$$\gamma_{\Lambda\Sigma^0}^{1(\eta)}=\frac{1}{\sqrt{3}}D^2\mu_u \tag{A4}$$

for the η loops.

The coefficients $\tilde{\gamma}_i^1$ evaluated from the graphs 3b are given, up to a factor of $-5\mathcal{C}^2/2$, by

$$\tilde{\gamma}_p^{1(\pi)}=-\frac{16}{9}\mu_u,\quad \tilde{\gamma}_{\Sigma^+}^{1(\pi)}=-\frac{1}{27}(5\mu_u+4\mu_s),$$

$$\tilde{\gamma}_{\Xi^0}^{1(\pi)}=-\frac{4}{9}\mu_s,$$

$$\tilde{\gamma}_n^{1(\pi)}=\frac{4}{9}\mu_u,\quad \tilde{\gamma}_{\Sigma^0}^{1(\pi)}=-\frac{2}{27}(\mu_u+2\mu_s),$$

$$\tilde{\gamma}_{\Xi^-}^{1(\pi)}=-\frac{1}{9}(\mu_u+4\mu_s),$$

$$\tilde{\gamma}_\Lambda^{1(\pi)}=-\frac{1}{3}(\mu_u+2\mu_s),\quad \tilde{\gamma}_{\Sigma^-}^{1(\pi)}=\frac{1}{27}(\mu_u-4\mu_s),$$

$$\tilde{\gamma}_{\Lambda\Sigma^0}^{1(\pi)}=-\frac{2}{3\sqrt{3}}\mu_u, \tag{A5}$$

for the pion loops, by

$$\tilde{\gamma}_p^{1(K)}=-\frac{1}{9}(3\mu_u+2\mu_s),\quad \tilde{\gamma}_{\Sigma^+}^{1(K)}=-\frac{2}{27}(23\mu_u+4\mu_s),$$

$$\tilde{\gamma}_{\Xi^0}^{1(K)}=-\frac{1}{9}(3\mu_u+14\mu_s),$$

$$\tilde{\gamma}_n^{1(K)}=\frac{1}{9}(\mu_u-2\mu_s),\quad \tilde{\gamma}_{\Sigma^0}^{1(K)}=-\frac{1}{27}(13\mu_u+8\mu_s),\tag{A6}$$

$$\tilde{\gamma}_{\Xi^-}^{1(K)}=\frac{1}{9}(\mu_u-14\mu_s),$$

$$\tilde{\gamma}_{\Lambda}^{1(K)}=-\frac{1}{9}(\mu_u+8\mu_s),\quad \tilde{\gamma}_{\Sigma^-}^{1(K)}=\frac{4}{27}(5\mu_u-2\mu_s),$$

$$\tilde{\gamma}_{\Lambda\Sigma^0}^{1(K)}=-\frac{1}{3\sqrt{3}}\mu_u,$$

for the kaon loops, and by

$$\tilde{\gamma}_p^{1(\eta)}=0,\ \tilde{\gamma}_{\Sigma^+}^{1(\eta)}=-\frac{2}{9}(2\mu_u+\mu_s),\ \tilde{\gamma}_{\Xi^0}^{1(\eta)}=-\frac{2}{9}(\mu_u+2\mu_s),\tag{A7}$$

$$\tilde{\gamma}_n^{1(\eta)}=0,\ \tilde{\gamma}_{\Sigma^0}^{1(\eta)}=-\frac{1}{9}(\mu_u+2\mu_s),\ \tilde{\gamma}_{\Xi^-}^{1(\eta)}=\frac{1}{9}(\mu_u-4\mu_s),$$

$$\tilde{\gamma}_{\Lambda}^{1(\eta)}=0,\ \tilde{\gamma}_{\Sigma^-}^{1(\eta)}=\frac{2}{9}(\mu_u-\mu_s),\ \tilde{\gamma}_{\Lambda\Sigma^0}^{1(\eta)}=0,$$

for the η loops.

The coefficients $\tilde{\gamma}_i^2$ evaluated from the graphs 3c (or 3d) are given, up to a factor of $2\mathcal{C}$, by

$$\tilde{\gamma}_p^{2(\pi)}=-\frac{8}{3}(D+F)\mu_u,\ \tilde{\gamma}_{\Sigma^+}^{2(\pi)}=-\frac{2}{9}((3D+5F)\mu_u-8F\mu_s),$$

$$\tilde{\gamma}_{\Xi^0}^{2(\pi)}=\frac{4}{3}(F-D)\mu_s,$$

$$\tilde{\gamma}_n^{2(\pi)}=\frac{8}{3}(D+F)\mu_u,\ \tilde{\gamma}_{\Sigma^0}^{2(\pi)}=-\frac{4}{9}F(\mu_u-4\mu_s),\tag{A8}$$

$$\tilde{\gamma}_{\Xi^-}^{2(\pi)}=\frac{2}{9}(D-F)(5\mu_u-2\mu_s),$$

$$\tilde{\gamma}_{\Lambda}^{2(\pi)}=\frac{2}{3}D(\mu_u-4\mu_s),\ \tilde{\gamma}_{\Sigma^-}^{2(\pi)}=\frac{2}{9}((3D+F)\mu_u+8F\mu_s),$$

$$\tilde{\gamma}_{\Lambda\Sigma^0}^{2(\pi)}=-\frac{1}{3\sqrt{3}}(D+6F)\mu_u$$

for the pion loops, by

$$\tilde{\gamma}_p^{2(K)}=-\frac{4}{3}[D\mu_u+(F-D)\mu_s],$$

$$\tilde{\gamma}_n^{2(K)}=\frac{2}{3}[(D+F)\mu_u+2(D-F)\mu_s],$$

$$\tilde{\gamma}_{\Lambda}^{2(K)}=\frac{2}{9}(3F-D)(\mu_u-4\mu_s),$$

$$\tilde{\gamma}_{\Sigma^+}^{2(K)}=\frac{4}{9}[(F-5D)\mu_u+2(D+F)\mu_s],\tag{A9}$$

$$\tilde{\gamma}_{\Sigma^0}^{2(K)}=-\frac{2}{9}(D+F)(\mu_u-4\mu_s),$$

$$\tilde{\gamma}_{\Sigma^-}^{2(K)}=\frac{8}{9}[(2D-F)\mu_u+(D+F)\mu_s],$$

$$\tilde{\gamma}_{\Xi^0}^{2(K)}=\frac{2}{3}[(D+3F)\mu_u-2(D+F)\mu_s],$$

$$\tilde{\gamma}_{\Xi^-}^{2(K)}=-\frac{4}{3}[F\mu_u+(D+F)\mu_s],$$

$$\tilde{\gamma}_{\Lambda\Sigma^0}^{1(K)}=-\frac{4}{3\sqrt{3}}(2D+3F)\mu_u,$$

for the kaon loops, and by

$$\tilde{\gamma}_p^{2(\eta)}=0,\ \tilde{\gamma}_{\Sigma^+}^{2(\eta)}=-\frac{8}{9}D(\mu_u-\mu_s),$$

$$\tilde{\gamma}_{\Xi^0}^{2(\eta)}=\frac{4}{9}(D+3F)(\mu_u-\mu_s),$$

$$\tilde{\gamma}_n^{2(\eta)}=0,\ \tilde{\gamma}_{\Sigma^0}^{2(\eta)}=-\frac{2}{9}D(\mu_u-4\mu_s),\tag{A10}$$

$$\tilde{\gamma}_{\Xi^-}^{2(\eta)}=-\frac{2}{9}(D+3F)(\mu_u+2\mu_s),$$

$$\tilde{\gamma}_{\Lambda}^{2(\eta)}=0,\ \tilde{\gamma}_{\Sigma^-}^{2(\eta)}=\frac{4}{9}D(\mu_u+2\mu_s),\ \tilde{\gamma}_{\Lambda\Sigma^0}^{2(\eta)}=-\frac{1}{\sqrt{3}}D\mu_u,$$

for the η loops.

APPENDIX B: THE EXPRESSIONS FOR L_0, $\tilde{F}$, L_1, AND L_2

Let us introduce the following notation

$$F_0(m,a)=\begin{cases}\sqrt{m^2-a^2}[\,\pi/2-\arctan(a/\sqrt{m^2-a^2})], & m\geqslant a,\\ -\sqrt{a^2-m^2}\,\ln[(a+\sqrt{a^2-m^2})/m], & m<a,\end{cases}\tag{B1}$$

where a is an arbitrary parameter. Hereafter, the subscript (X) is ignored. The function $L_0(m,\lambda)$ obtained from the Feynman integral for the graph 3a (or 3e) is then given by

$$L_0(m,\lambda)=\frac{\lambda^4}{(\lambda^2-m^2)^2}\left(\frac{1}{3}(\lambda^2+2m^2)+\frac{\lambda m^2}{\lambda^2-m^2}F_0(m,\lambda)\right). \tag{B2}$$

The function $\tilde{F}(m,\delta,\lambda)$ obtained when calculating a Feynman integral for the graph 1b is

$$\begin{aligned}\pi\tilde{F}(m,\delta,\lambda)=&-\frac{\lambda^4}{3(\lambda^2-m^2+\delta^2)^2}\Bigg[N(m,\delta,\lambda)\\&+\frac{5\lambda^2+2m^2}{\lambda^2-m^2}\delta+\frac{\lambda^2+2m^2}{(\lambda^2-m^2)^2}\delta^3\\&+\frac{\lambda\delta}{(\lambda^2-m^2)^2(\lambda^2-m^2+\delta^2)}\Bigg(3(2\lambda^2+3m^2)\\&\times(\lambda^2-m^2)-2(\lambda^2-6m^2)\delta^2\\&+\frac{3m^2}{\lambda^2-m^2}\delta^4\Bigg)F_0(m,\lambda)\Bigg],\end{aligned} \tag{B3}$$

where

$$\begin{aligned}N(m,\delta,\lambda)=&\frac{1}{(\lambda^2-m^2+\delta^2)}\left[\pi\lambda(\lambda^2+3m^2-3\delta^2)\right.\\&\left.-2(3\lambda^2+m^2-\delta^2)F_0(m,\delta)\right].\end{aligned} \tag{B4}$$

Similarly, the functions $L_1(m,\delta,\lambda)$, and $L_2(m,\delta,\lambda)$ arise from the Feynman integrals for the graphs 3b (or 3f) and 3c (or 3d), respectively. We have

$$\begin{aligned}L_1(m,\delta,\lambda)=&\frac{2\lambda^4}{3(\lambda^2-m^2+\delta^2)^2}\Bigg[(\lambda^2+2m^2-2\delta^2)\\&-\delta N(m,\delta,\lambda)-\frac{\lambda^2}{\lambda^2-m^2}\delta^2\\&+\frac{\lambda}{(\lambda^2-m^2)(\lambda^2-m^2+\delta^2)}\\&\times\Bigg(3m^2(\lambda^2-m^2)-6\lambda^2\delta^2\\&+\frac{2\lambda^2-3m^2}{\lambda^2-m^2}\delta^4\Bigg)F_0(m,\lambda)\Bigg],\end{aligned} \tag{B5}$$

and

$$\begin{aligned}&L_2(m,\delta,\lambda)\\&=-\frac{2\lambda^4}{3(\lambda^2-m^2+\delta^2)^2}\Bigg[\left[2(m^2-\delta^2)F_0(m,\delta)-\pi m^3\right]\frac{1}{\delta}\\&+\frac{\pi\delta}{2(\lambda+m)}\left((\lambda^2+\lambda m+4m^2)-\frac{\lambda+2m}{\lambda+m}\delta^2\right)\\&-\frac{\lambda^2(\lambda^2-m^2+\delta^2)}{\lambda^2-m^2}-\frac{\lambda}{(\lambda^2-m^2)^2}\\&\times\left[3m^2(\lambda^2-m^2)-(2\lambda^2-3m^2)\delta^2\right]F_0(m,\lambda)\Bigg].\end{aligned} \tag{B6}$$

When $\delta=0$, Eq. (B3) gives

$$\tilde{F}(m,0,\lambda)=-\frac{\lambda^4}{3(\lambda+m)^3}, \tag{B7}$$

and it follows from Eqs. (B5) and (B6) that

$$\begin{aligned}L_1(m,0,\lambda)=L_2(m,0,\lambda)&=2L_0(m,\lambda)\\&=\frac{2\lambda^4}{3(\lambda^2-m^2)^2}\left((\lambda^2+2m^2)\right.\\&\left.+\frac{3\lambda m^2}{\lambda^2-m^2}F_0(m,\lambda)\right).\end{aligned} \tag{B8}$$

[1] L. Durand and P. Ha, Proceedings of the Como Conference on Quark Confinement and Hadron Spectrum II, edited by N. Brambilla and G. M. Prosperi (World Scientific, Singapore, 1996).

[2] E. Jenkins, M. Luke, A. V. Manohar, and M. Savage, Phys. Lett. B **302**, 482 (1993); **388**, 866(E) (1996).

[3] M. A. Luty, J. March-Russell, and M. White, Phys. Rev. D **51**, 2332 (1995).

[4] J. Dai, R. Dashen, E. Jenkins, and A. V. Manohar, Phys. Rev. D **53**, 273 (1996).

[5] Ulf-G. Meißner and S. Steininger, Nucl. Phys. **B499**, 349 (1997).

[6] J. W. Bos, D. Chang, S. C. Lee, Y. C. Lin, and H. H. Shih, Chin. J. Phys. (Taipei) **35**, 150 (1997). J. W. Bos, D. Chang, S. C. Lee, and H. H. Shih, hep-ph/9702272.

[7] L. Durand and P. Ha, Phys. Rev. D **58**, 013010 (1998).

[8] S. Coleman and S. L. Glashow, Phys. Rev. Lett. **6**, 423 (1961).

[9] H. Georgi, Phys. Lett. B **240**, 447 (1990).

[10] E. Jenkins and A. V. Manohar, Phys. Lett. B **255**, 558 (1991); **259**, 353 (1991); Report No. UCSD/PTH 91-30.

[11] N. Brambilla, P. Consoli, and G. M. Prosperi, Phys. Rev. D **50**, 5878 (1994).
[12] J. Carlson, J. Kogut, and V. R. Pandharipande, Phys. Rev. D **27**, 233 (1983); **28**, 2807 (1983).
[13] S. Capstick and N. Isgur, Phys. Rev. D **34**, 2809 (1986).
[14] A. Krause, Helv. Phys. Acta **63**, 3 (1990).
[15] J. Donoghue and B. R. Holstein, hep-ph/9803312.
[16] P. Ha, Phys. Rev. D (to be published), hep-ph/9804383.
[17] A. Bincer, Phys. Rev. **118**, 855 (1960).